



# HHS Public Access

Author manuscript

*Adv Funct Mater.* Author manuscript; available in PMC 2020 August 07.

Published in final edited form as:

*Adv Funct Mater.* 2018 March 21; 28(12): . doi:10.1002/adfm.201702009.

## A Dual-layered Microfluidic System for Long-term Controlled In Situ Delivery of Multiple Anti-inflammatory Factors for Chronic Neural Applications.

**Laura Frey,**

Biomaterials Innovation Research Center, Division of Engineering in Medicine, Department of Medicine, Brigham and Women's Hospital, Harvard Medical School, Boston, MA 02139, USA.

Harvard-MIT Division of Health Sciences and Technology, Massachusetts Institute of Technology, Cambridge, MA 02139, USA.

Trinity Centre of Bioengineering, Trinity College Dublin, Dublin 2, Ireland.

**Praveen Bandaru,**

Biomaterials Innovation Research Center, Division of Engineering in Medicine, Department of Medicine, Brigham and Women's Hospital, Harvard Medical School, Boston, MA 02139, USA.

Harvard-MIT Division of Health Sciences and Technology, Massachusetts Institute of Technology, Cambridge, MA 02139, USA.

**Yu Shrike Zhang,**

Biomaterials Innovation Research Center, Division of Engineering in Medicine, Department of Medicine, Brigham and Women's Hospital, Harvard Medical School, Boston, MA 02139, USA.

Harvard-MIT Division of Health Sciences and Technology, Massachusetts Institute of Technology, Cambridge, MA 02139, USA.

Wyss Institute for Biologically Inspired Engineering, Harvard University, Boston, MA 02115, USA.

**Kevin O'Kelly\***

Biomaterials Innovation Research Center, Division of Engineering in Medicine, Department of Medicine, Brigham and Women's Hospital, Harvard Medical School, Boston, MA 02139, USA.

Harvard-MIT Division of Health Sciences and Technology, Massachusetts Institute of Technology, Cambridge, MA 02139, USA.

Trinity Centre of Bioengineering, Trinity College Dublin, Dublin 2, Ireland.

**Ali Khademhosseini\***

Biomaterials Innovation Research Center, Division of Engineering in Medicine, Department of Medicine, Brigham and Women's Hospital, Harvard Medical School, Boston, MA 02139, USA.

Harvard-MIT Division of Health Sciences and Technology, Massachusetts Institute of Technology, Cambridge, MA 02139, USA.

---

okellyk@tcd.ie (Kevin O'Kelly), alik@bwh.harvard.edu (Ali Khademhosseini), sshin4@partners.org (Su Ryon Shin).

\*These authors contributed equally as corresponding authors to this work.

Wyss Institute for Biologically Inspired Engineering, Harvard University, Boston, MA 02115, USA.

**Su Ryon Shin\***

Biomaterials Innovation Research Center, Division of Engineering in Medicine, Department of Medicine, Brigham and Women's Hospital, Harvard Medical School, Boston, MA 02139, USA.

Harvard-MIT Division of Health Sciences and Technology, Massachusetts Institute of Technology, Cambridge, MA 02139, USA.

Wyss Institute for Biologically Inspired Engineering, Harvard University, Boston, MA 02115, USA.

**Abstract**

We report the development of a microfluidic system capable of repeated infusions of anti-inflammatory factors post-implantation for use as a coating for neural probes. This system consists of a microchannel in a thin gelatin methacryloyl (GelMA)-polyethylene glycol (PEG) composite hydrogel surrounded by a porous polydimethylsiloxane (PDMS) membrane, where the hydrogel can be dried to increase the stiffness for easy insertion. Reswelling allowed us to perfuse interleukin (IL)-4 and dexamethasone (DEX) as anti-inflammatory factors through the channel with minimal burst release and significant amounts of IL-4 were observed to release for up to 96 hr post-infusion. Repeated injections of IL-4 increased the ratio of prohealing M2 *versus* proinflammatory M1 phenotypes of macrophages encapsulated in the hydrogel by six fold compared with a single injection, over a 2-week period. These repeated infusions also significantly downregulated the expression of inflammatory markers tumor necrosis factor (TNF)- $\alpha$  and IL-6 in astrocytes encapsulated in hydrogel. To demonstrate the system as a coating of neural probe for *in vivo* applications, we further fabricated a prototype device, where a thin dual-layered microfluidic system was integrated onto a metal probe. Such a drug delivery system could help reduce the formation of a glial scar around neural probes.

**Keywords**

Microfluidic system; Hydrogel; Drug delivery; Neural probes; Neural electrodes; Astrocytes

**1. Introduction**

In recent years, considerable advances have been made regarding the use of neural electrodes to not only measure and record brain functionality, but to suppress or stimulate different areas of the brain in order to treat a variety of conditions<sup>[1]</sup>. These electrodes have been successfully employed to minimize the effects of motor neuronal disease<sup>[2]</sup>, Parkinson's disease<sup>[3]</sup>, epilepsy<sup>[3a, 3b, 4]</sup> and to overcome the effects of paralysis<sup>[1b, 5]</sup>. Furthermore, advancements are being made in the use of electrodes to combat deafness and blindness through cochlear and retinal implants and to reduce the effects of mood disorders by deep brain stimulation (DBS) <sup>[3-4]</sup>.

The short-term successes of these implants are well-documented with DBS now being a U.S. Food and Drug Administration (FDA)-approved treatment for dystonia, Parkinson's, and essential tremor in the US<sup>[1c]</sup>. However, there have been challenges with long-term utilization of these electrodes. Sometimes positive initial results and reductions in symptoms

reduce over time as the electrodes become less effective [1b, 6]. This reduction in effectiveness is usually attributed to the gradual encapsulation of the electrode by scar tissues and therefore the issue cannot be dealt with by simply replacing an electrode. This can be attributed to the initial insertion-associated injury (acute response)<sup>[7]</sup>, presence of a foreign material (chronic response)<sup>2,15</sup>, damage caused by micro-motion of the inserted electrode<sup>[1a],[3c, 8]</sup>, or repeated electrical over-stimulation of the tissue<sup>[9]</sup>. For these reasons, much of the research has focused on making the electrodes as small and biocompatible as possible, with recent research also highlighting the importance of matching biomechanical properties.

Several recent studies have shown that strategies that effectively reduce the acute anti-inflammatory response to implants often are indistinguishable from untreated devices at the chronic stage of implantation. For example, a study by Potter *et al*<sup>[10]</sup> where neural implants released curcumin from polyvinyl alcohol film coatings over time, with most of the release occurring in the first 10 hours, showed a reduction in scar tissue and an increase in functioning neurons surrounding the implant at 4 weeks. However, once 12 weeks was reached, there was no statistical difference between the implants which were drug-eluting and those that were not. Although not a drug-eluting probe, the same phenomena was found when investigating the shape and size effects on glial scarring in a study by Szarowski *et al*<sup>[8a]</sup>. Smaller rounded implants showed a reduction in the acute response of microglia (defined as less than 2 weeks in this study) but chronic results from 4 weeks to up to 12 weeks showed no significant difference between all designs<sup>[8a]</sup>.

These studies indicate that, in order to create viable probes for long-term implantation, a strategy to reduce the inflammatory reaction of the brain tissue in its chronic phase is required. The definition of chronic itself is up for debate, with many studies not defining what they deem to be chronic at all, or suggestions ranging from 1 to 12 weeks with most settling around the 2–4 week mark [11]. For this study, an chronic phase is considered as 2 weeks or greater as this has been indicated to be the transition point [12]. This study thus considered the design and optimization of a dual-layered microfluidic system that would allow for long-term and steady delivery of an optimized profile of anti-inflammatory drugs and cytokines over a period of at least 2 weeks, with the potential to increase past that point if required. It was hypothesized that being able to sustain this delivery and change the factor being delivered would significantly reduce the inflammatory reaction of macrophages and astrocytes, leading to a reduction in scar tissue formation and a probe that functions better long-term. Tests were performed on both macrophages as they form the initial response to an injury, as well as astrocytes as they also release inflammatory factors, and they make up 30–65% of glial cells in the brain and are the predominant cell within the glial scar [1b]. As both cells therefore play a significant role in immune reaction and scar formation it was important to assess both reactions to sustained release of anti-inflammatory factors in order to strengthen any findings [13]. THP-1 monocytes are used to form the macrophage model as these cells are widely used in inflammation studies. These cells have also been shown to exhibit similar inflammatory responses to microglia *in vivo* and blood-derived macrophages will also infiltrate upon probe insertion. In addition, the behavior of these macrophages correlates strongly with neuronal loss, a big concern for neuronal probe application [14]. For this study we chose not to look at the response of neurons themselves as this is often

dependent on the glial response and it is difficult to maintain primary neurons chronically *in vitro*<sup>[15]</sup>. The response of neurons themselves will be assessed at the following *in vivo* stage in our future studies that has already been planned.

Furthermore, the dual layer system was to involve a drying stage to minimize the size and increase the stiffness of the implant for easy insertion in future clinical applications. It would also allow reswelling of the coating on insertion, which could reduce the damage to the surrounding tissue caused by micro-motion of the electrode as well as making the electrode surface more mechanically compliant and similar to brain tissue. In order to ensure that the mechanical integrity of the microchannels was maintained during this cycle, and would be better sustained throughout implantation, reswelling tests were carried out and the effects of the addition of PEG to the GelMA layer to create a mechanically robust hydrogel was investigated. These hypotheses were tested by optimizing the design of the dual-layered coating in the chip form and assessing the diffusion profile of differently sized molecules representing anti-inflammatory drugs through this dual-layered chip system. Once a final design was reached, the effect on macrophages and astrocytes of sustained release, from this dual-layered system, of dexamethasone (DEX) as an anti-inflammatory drug and interleukin-4 (IL-4) as an anti-inflammatory cytokine *versus* a single infusion of both factors over a 3-week period was investigated. The comparison *versus* single infusions through the dual layered system was important to highlight that any additional improvements were coming from the system's ability to sustain delivery of the factors throughout the acute and into the chronic phase of immune response. In order to keep macrophages and astrocytes alive and representative of *in vivo* conditions, their surrounding environment was important, therefore for both cells an optimization stage for their GelMA conditions was included to ensure the cells were initially in as resting a state as possible. As a proof of concept for future *in vivo* application, a thin dual-layered microfluidic device with hydrogel coating on the inner walls of the microchannel was fabricated and characterized for the diffusion profile of fluorescein isothiocyanate (FITC)-dextran.

## 2. Results and Discussion

### 2.1 Fabrication of Microchannel in Hydrogel

To fabricate a microchannel, we selected gelatin methacryloyl (GelMA) hydrogel that has been shown to support the growth of a wide variety of cells when the cells are either in contact with its surface or encapsulated within its structure<sup>[16]</sup>. It is also an enabling material for drug delivery applications as its porous structure can be fine-tuned to control the rate of drug release into the surrounding environment<sup>[17]</sup>. By optimizing the photocrosslinking time, mechanical properties of the gel can also be exploited to easily fabricate and retain microchannels within the structure. However, particularly at lower concentrations, GelMA hydrogel can degrade quickly over time and diffusion through the gel can be quick<sup>[17b]</sup>. For these reasons, as well as preventing excessive reswelling post-insertion and allowing even greater control over the drug release, a porous polydimethylsiloxane (PDMS) membrane layer was further added to the GelMA hydrogel containing the microchannel. PDMS is also non-toxic and non-biodegradable<sup>[18]</sup> and the

reduced surface area for diffusion through the hydrogel-based microfluidic system could further slow down the release of active molecules.

The concept and process for fabricating this system is illustrated in Figure 1. During the developmental process it was noticed that the drying and reswelling stages were having an adverse effect on the integrity of the hydrogel, particularly if they were left for more than 3 days in the dry state. The crosslinking of PEG and GelMA chains was to provide resistance to cracking upon drying by increasing the density of polymeric networks, resulting in improved mechanical strength of the composite hydrogel, similar to the result of composite hydrogel reported in our previous work<sup>[19]</sup>. The acryloyl substitution groups on the GelMA and PEGDA chains were covalently bounded after UV exposure resulting in a GelMA/PEG composite hydrogel. For this reason, three different hydrogel formulations were investigated: 5% GelMA, 10% GelMA, and 10% GelMA/2% PEG. First, their mechanical properties with varying degrees of photocrosslinking post-drying and reswelling were analyzed. The compressive moduli of 5% GelMA, 10% GelMA, and 10% GelMA/2% PEG hydrogel were  $2.83 \pm 0.40$  kPa,  $3.26 \pm 0.45$  kPa, and  $6.41 \pm 0.67$  kPa, respectively (Fig. 2A). As the compressive modulus of the brain tissue is around 1 kPa<sup>[20]</sup> all of these formulations are strong enough to resist deformation by the brain tissue itself while not being so stiff that they cause a mechanical mismatch between the implant surface and the brain, which has been shown to increase the brain's immune reaction to implants<sup>[21]</sup>. The reswelling profiles of the three formulations were also assessed in order to ascertain if they would exert undue pressure on the brain and if their reswell time had the potential to be problematic in surgery as sometimes implants have to be removed and reinserted several times during this time<sup>[22]</sup>. All three formulations had similar reswelling profiles with total reswell within 4 hours in phosphate buffered saline (PBS, Fig. 2B). The thicknesses of the gels in their dry state were  $210 \pm 40$   $\mu\text{m}$ ,  $430 \pm 20$   $\mu\text{m}$ , and  $350 \pm 20$   $\mu\text{m}$ , respectively. After 72 hr of drying in air, the 10% GelMA/2% PEG hydrogel was the only formulation that remained entirely crack free among all samples. For this reason, as well as its thickness of only  $350 \pm 20$   $\mu\text{m}$  in the dry state, this formulation was chosen for fabrication of the device. Scanning Electron Microscopy (SEM) images taken of this hydrogel (Fig. 2C) show the porous structure of the gel with pores of to  $90 \pm 37$   $\mu\text{m}$  in diameter. The device itself was designed as a square piece with one single cylindrical microchannel of  $80 \pm 16$   $\mu\text{m}$  through the hydrogel in order to simplify verification of the diffusive gradient (Fig. 2D). In practice however, the channel would be a loop to allow easier filling and emptying of the channel and this was also fabricated in order to show that this loop structure would be possible in the future. The appearance of the device itself as well as the microchannel and porous PDMS membrane under the microscope are shown in Fig. 2E–H with the hydrogel stained green.

## 2.2 Diffusion through the Scaffold

To evaluate the diffusion of potential anti-inflammatory factors such as drug and interleukins through our system, FITC-dextran with various molecular weights ( $M_W$ ) were used. DEX is a commonly used anti-inflammatory drug, particularly at the acute stage of inflammation and has a  $M_W$  of 392 Da<sup>[15, 23]</sup>. FITC isomer has a  $M_W$  of 389 Da and has been used as a model for DEX. Interleukins are a family of cytokines involved in the inflammatory process and some of these such as IL-4 have been shown to have anti-inflammatory effects<sup>[24]</sup>. IL-4

has a  $M_W$  in the range of 12–20 kDa, and therefore FITC-dextran with 20-kDa was chosen as a model for this cytokine, with tests also conducted with 40-kDa FITC-dextran as a model for larger proteins that may be investigated at a later stage. In order to evaluate the diffusion of these FITC-based molecules, sample dual layered microfluidic chips were placed under the fluorescent microscope and a single injection of the substance was added to the microchannel (Fig. 3A (i)). The channel and its surrounding gel area were imaged every 2 min until the dye had diffused throughout the chip (Fig. 3B). The fluorescence intensity was significantly decreased by increasing the  $M_W$  of FITC variants and then decreased after saturation by diffusion of FITC variants through the hydrogel (Fig. 3C).

The diffusion of the anti-inflammatory factors through the whole chip including the porous PDMS membrane and into the brain tissue on the other side is actually more relevant to our studies as this will allow us to specifically target different points in the inflammatory process with our molecules in future. This was evaluated by adding a PBS reservoir on top of the chip into which the FITC variants could diffuse over time (Fig. 3A (ii)). Samples from this PBS reservoir could then be measured for fluorescence at regular intervals and the entire PBS reservoir replaced to maintain sink conditions as would be present in the brain. The obtained intensity of fluorescence signals were correlated to the concentrations of the FITC variants using the calibration curves of each FITC variants. Concentration of the FITC variants was plotted against time at 24-hr intervals to identify peak release from the system and to assess the release profile (Fig. 3D). 40-kDa FITC-dextran had its peak release at 48 hr while both 20-kDa and 40-kDa FITC-dextran could be released from the system for up to 4 days after the initial infusion through the microchannel. This delayed peak release could be utilized when trying to release factors at precise stages of inflammation reaction for an optimized drug delivery profile in future. As the release of FITC isomer and 20-kDa FITC-dextran both peaked at 24 hr or before, the experiment was repeated with 8 hr time points (Fig. 3E). This showed the initial release of the 20-kDa FITC-Dextran was steady over the first 24 hr and there was minimal burst release of the FITC isomer, a common problem with drug delivery systems<sup>[10]</sup>. These results showed an interesting contrast to the diffusion behavior of FITC variants through the hydrogel previously (Fig. 3C), where the diffusion of 20- and 40-kDa FITC-dextran were not significantly different. This may be due to the addition of the porous PDMS membrane that was further slowing down the diffusion of dextran into the PBS reservoir. These findings resulted in the decision to diffuse molecules twice a week for future chronic cell trials to ensure that cells would have a constant supply of our anti-inflammatory factors delivered to them.

### 2.3 Monocyte Model Development and Chronic Drug Study

Once the drug delivery chip had been designed and optimized, a model for the brain was developed (Fig. 4). As microglia are the first response to any injury in the brain, moderating their response can affect the whole chain of inflammation events<sup>[13a]</sup>. Microglia are sometimes referred to as the macrophages of the brain as they carry out many of the same duties that macrophages carry out in the rest of the body<sup>[25]</sup>. Microglia are difficult to harvest and purify without having other remaining cell types whereas macrophages can be formed from monocytes using a well-established cell line THP-1. As both macrophages and microglia have the ability to differentiate into M1 or M2 phenotypes, which correspond to

pro-inflammatory and anti-inflammatory macrophages, respectively, monocytes represent a suitable model for investigating the effects of a drug delivery profile on the brain<sup>[26]</sup>. In order to create a more brain-like environment and allow longer survival of the cells, GelMA hydrogel was used as a three-dimensional (3D) scaffold to imitate the brain-like extracellular matrix (ECM). The photocrosslinkable nature of this hydrogel allowed the fine-tuning of the mechanical properties to mimic brain tissue as 20-s UV light exposure resulted in a compressive modulus of  $1.27 \pm 0.17$  kPa, which is similar to the brain tissue (Fig. 4A)<sup>[20]</sup>. Live/dead analysis of the encapsulated monocytes at these conditions was carried out at days 0 and 7 of encapsulation without drug delivery treatment (Fig. 4B and C). The live cells are shown in green and the red indicates dead cells, indicating over 90% cells remaining viable at day 0 and over 80% at day 7.

Different test conditions for the drug delivery profile were designed and performed (Fig. 4D). The profiles chosen consisted of a negative control with no infusions, an initial DEX infusion with subsequent twice per week DEX infusions, a single IL-4 infusion, an initial DEX infusion with subsequent twice per week IL-4 infusions, and an initial IL-4 infusion and subsequent twice per week IL-4 infusions (Table S1, supplementary information). All infusions were injected directly into the dual-layered microfluidic chip, upon which a macrophage-laden hydrogel was placed in order to simulate delivery from a probe coating into the brain. When quantifying the ratio of cells with M2 (green) anti-inflammatory *versus* M1 (red) pro-inflammatory phenotypes, the negative control showed an increase from week 1 to week 2 without any infusion of anti-inflammatory factors, implying that the chips themselves do not have an adverse effect on the cells (Fig. 4E–I and J). At week 2, the negative control statistically had the same ratio of M2:M1 cells as the samples with only one infusion of IL-4 and was performing better than those with repeated injections of DEX. Due to the use of a high concentration of DEX (0.1 mg/ml: ~333 nM)<sup>[27]</sup> compared with previously reported studies that used 10 nM or 100 nM DEX to induce M2 macrophage polarization<sup>[28]</sup>, it may have induced cytotoxicity during infusion of DEX to the monocyte model. By week 2 both conditions that involved repeated injections of IL-4 resulted in significantly increased ratios of M2:M1 macrophages, with the samples of IL-4 initial and IL-4 follow-up injections increasing the ratio 6-fold compared with the negative control at the same time point (Fig. 4J). This increase in M2 macrophages as a result of IL-4 stimulation was also observed for macrophages directly seeded onto IL-4-incorporated poly-L-lysine/hyaluronic composite films, along with a reduction in expression of inflammatory cytokines TNF- $\alpha$ , IL-12, and IL-1 $\beta$ <sup>[29]</sup>. In order to strengthen these findings in the next stage we repeated the tests with primary astrocytes (the main cell type in a glial scar) and carried out immunoassays for released inflammatory cytokines.

## 2.4 Development of Brain-like Tissue Model and Chronic Study for Astrocyte Model

3D astrocyte models are advantageous as, without a matrix to support their growth and network formation, the cells will die within a few days, and therefore chronic studies cannot be carried out<sup>[30]</sup>. These 3D models are also a more accurate representation of the brain structure. In order to form networks, astrocytes need a precise extracellular environment, and otherwise the cells would stay circular and die without behaving as astrocytes would *in vivo*<sup>[30]</sup>. For this reason, a variety of different percentages of photoinitiator (PI) and UV

exposure time were tested in order to find the optimum parameters for healthy network formation. An initial screening immediately eliminated some combinations for being too weak to properly encapsulate cells and survive long term in an *in vitro* environment (Table S2, supplementary information). The promising combinations had cells encapsulated in 600- $\mu\text{m}$  thick hydrogels, leaving cells to survive *in vitro* for a week for them to extend their processes and make connections with each other. These hydrogels were then imaged up to 200  $\mu\text{m}$  deep into the structure so that a 3D representation of the cells could be built up. Neither 20-s UV/0.5% PI and 40-s UV/0.5% PI were suitable with very few cells having outgrowth and a lot of cell death apparent (Fig. S1A and B). 30-s UV/0.5% PI and 40-s UV/0.3% PI both showed some cell network formation but also many round dead cells (Fig. S1C and D). The optimum conditions for cell network formation were found to be the hydrogel with 0.3% PI and 30-s UV exposure as the majority of the cells had outgrowth with multiple connections and strong networks (Fig. S1E). The cross-section of the 3D image shows how this network spreaded throughout the entirety of the hydrogel and for this reason these conditions were chosen for the astrocyte model to test our drug delivery profiles (Fig. 5A).

To test chronic drug delivery for the *in vitro* astrocyte model, we applied drugs with different delivery profiles (Table S3, supplementary information) similar with the chronic study for the monocyte model. By the end of 3 weeks, both the negative control and the samples with DEX injections only had some astrocytes with long extended processes but no evidence of a strong network of cells (Fig. 5B and C). The samples with a single injection of IL-4 showed an increased number of live cells with the formation of a more substantial network (Fig. 5D). However, the samples with repeated IL-4 injections clearly had the healthiest networks of astrocyte cells (Fig. 5E and F). ELISA immunoassays were also used to calculate the expression of inflammatory markers from the cell encapsulated hydrogels at week 1 and week 3. TNF- $\alpha$  is often viewed as the most consistent and unambiguous marker for cell inflammation<sup>[31]</sup> and its release from samples was measured at week 1 and week 3 (Fig. 5G). There was no significant difference between samples at 1 week and 3 weeks, indicating that inflammation is stable throughout this period. The negative control had significantly increased inflammation *versus* those with a single IL-4 injection, DEX and a repeated IL-4 injection, and IL-4 repeated injections only with p values of 0.03, 0.0004, and 0.0002, respectively. Repeated DEX injections did not cause significant changes in inflammation *versus* the negative control or the IL-4 single injection; however, both DEX (p=0.02 and p=0.03) and IL-4 single injections (p=0.01 and p=0.02) had significantly higher amounts of TNF- $\alpha$  released than that of the repeated IL-4 injections. There was no significant difference in the repeated IL-4 injections between those injected with DEX or IL-4 initially, which implies that it is the repeated nature of IL-4 injections causing the reduction in inflammation over the 3-week period.

IL-6 is another marker of inflammation and its expression was also measured at 1 and 3 weeks (Fig. 5H). There were no significant changes in inflammation between the negative control, the repeated DEX injections, or the IL-4 single injection. All samples with repeated IL-4 injections had significantly reduced release of IL-6 *versus* the negative control (p=0.01 and 0.003) or the repeated DEX injected samples (p=0.04 and p=0.002). Interestingly, there was no significant difference between any of the repeated IL-4 injections or a single IL-4



injection, implying that the first few days of inflammation may be the most significant when it comes to releasing IL-6. Overall, both TNF- $\alpha$  and IL-6 release data show that repeated injections of IL-4 could be used to reduce the inflammatory response of the brain tissue to an electrode over time, although it must be noted that TNF- $\alpha$  expression did still slightly increase between weeks 1 and 3.

## 2.5 Development of Thin Dual-layered Microfluidic System on the Metal Probe

To prove the possibility of the usage of the coating for delivery of anti-inflammatory molecules on the neural probe for future *in vivo* evaluation, we further developed a thin microfluidic device (thickness:  $\sim 600\ \mu\text{m}$ ) containing a 10% GelMA/2% PEG composite hydrogel microchannel and integrated it to one side of a metal probe ( $450\ \mu\text{m}$  in diameter) (Fig. 6A). The microchannel with  $\sim 5.5\ \text{cm}$  in length,  $\sim 150\ \mu\text{m}$  in height, and  $\sim 120\ \mu\text{m}$  in width was fabricated using an SU-8 mold and then covered by a thin porous PDMS membrane with  $200\text{-}\mu\text{m}$  pores and  $100\text{-}\mu\text{m}$  thickness. The fabricated thin microchannel was easily bonded to one side of the metal probe using additional PDMS, leading to a total thickness of whole construct of  $\sim 1.5\ \text{mm}$  similar to that of current DBS electrodes in the market and therefore a clinically viable option (Fig. 6A). Although some research shows that decreasing the size of electrodes reduces the inflammatory response [32], alternative studies indicate that although the acute response is reduced, this often is not witnessed in long term [11a]. However, mechanical injury should be assessed *in vivo* at a later stage.

To create the hydrogel layer, 10% GelMA/2% PEG pre-polymer solution was flown through the microchannel while being exposed to UV light for crosslinking GelMA and PEG. GelMA/PEG composite hydrogel was uniformly coated on the inner wall of the microchannel with  $\sim 30\text{-}\mu\text{m}$  thickness as shown in Fig. 6B. The thickness of the GelMA/PEG coating in the microchannel however, could potentially be controlled by flow rate and concentration of the pre-polymer solution and UV exposure time [33]. To confirm the diffusion of anti-inflammatory drugs through the GelMA hydrogel coating and the porous PDMS membrane in the thin microfluidic device, FITC-dextran with  $20\text{-kDa}\ M_w$  was perfused through the microchannel and imaged at various intervals (Fig. 6C). Fluorescence intensity quantified at the central portion of the channel displayed the profile of the formation of the FITC-dextran gradient and the normalized average distance FITC-dextran diffused (Fig. 6D and E). In addition, the rate of diffusion *via* the thin microfluidic device could be controlled by changing the composition of the coating hydrogel. The thin microfluidic device coated by the 14% GelMA hydrogel showed faster diffusion of FITC-dextran with  $20\text{-kDa}\ M_w$  than that of GelMA/PEG-coated device (Fig. S3). It was clear that this microfluidic setup provided a uniform diffusion profile through the GelMA/PEG coating and the porous PDMS membrane, indicating its potential translation for *in vivo* applications in the future.

## 3. Conclusions

A dual layered microfluidic system was developed for use as a coating for neural electrodes which could be inserted in a thin dry state and then be held firmly in place by its own reswelling, protecting the brain against damage caused by micromotion of the electrode. The

system can easily be infused with a range of anti-inflammatory factors at body temperature for a period of at least three weeks without degradation and this profile of infusion has the potential to be fine-tuned to target specific phases of the brain's immune reaction. The system allows the steady release of cytokines for at least four days from one infusion and has a minimal burst release of small molecules. In order to assess the potential anti-inflammatory effects of factors delivered through the designed dual layered microfluidic system, a number of glial cell models were developed and optimized, before using the chip to deliver factors and measure their effect upon the cells. Therefore, two different hydrogels with optimized cell-specific mechanical properties encapsulated with either monocytes or astrocytes were developed as brain-like models and these hydrogels were able to last in an *in vivo*-mimicking environment for a minimum of 2 and 3 weeks, respectively. The repeated infusion of IL-4 caused both an upregulation in M2-induced macrophages over 2 weeks and a down regulation of both TNF- $\alpha$  and IL-6 in astrocytes over a 3-week period. Further work could involve the development of an encapsulated co-culture of microglia and astrocytes as a more realistic model for the brain *in vitro*. DEX infusion had no effect on either of these measured outputs, however, further work must be done to assess the mechanisms of DEX's the anti-inflammatory effects of dextran as these are well recognized elsewhere in the body. These improvements in anti-inflammatory effects *in vitro* imply that repeated infusions of anti-inflammatory factors like IL-4 could be utilized in the future to reduce the formation of a glial scar around neural implants and increase their efficacy long-term. A thin dual-layered microfluidic device with GelMA/PEG coating on the inner walls of the microchannel and a porous PDMS membrane, wrapped on a metal probe, was also fabricated for the proof of concept demonstration of the delivery of anti-inflammatory molecules through GelMA/PEG coating from a neural probe. This thin microfluidic system can be coated onto or be embedded in neural probes for *in situ* delivery of multiple anti-inflammatory factors for future *in vivo* evaluations, with a focus on the cellular and vascular structures at the probe-tissue interface for periods of time of 3 weeks and greater. The system may also find other potential drug delivery applications in the wider implant and medical device industry that are being explored.

## 4. Experimental Methods

### 4.1. Synthesis of Gelatin Methacryloyl (GelMA)

Gelatin from porcine skin (Sigma-Aldrich) was dissolved at 10% (w/v) in 100ml phosphate buffered saline (PBS) at 50 °C for 1 hr<sup>[34]</sup>. Next, 8 ml methacrylic anhydride (Sigma Aldrich) was slowly added to the gelatin solution and stirred at 50°C for 2 hr before an additional 100 mL of PBS was added and mixed at 50°C in order to stop the reaction. The obtained solution was dialyzed at 40 °C for 7 days using dialysis membranes ( $M_w$  cut off: 12–14 kDa, Fisher Scientific). The purified solution was filtered using a vacuum filtration cup with 0.22- $\mu$ m pores (Millipore). This solution was frozen to –80 °C before freeze drying for 5 days.

### 4.2. GelMA Solutions

Pre-polymer solutions of 5% GelMA for cell encapsulation were prepared with 0.5% PI (2-hydroxy-1-(4-(hydroxyethoxy) phenyl)-2-methyl-1-propanone 98%, Sigma Aldrich) in PBS.

For scaffold manufacture, 10% GelMA, 2% PEG diacrylate (PEGDA) (1000 M<sub>w</sub>, Polysciences), 0.5% PI solutions were used. All UV crosslinking was carried out at 6.9 mW/cm<sup>2</sup>.

#### 4.3. Fabrication of PDMS Membranes

All PDMS was prepared at a ratio of 10:1 with its curing agent (Sylgard 184 Silicone Elastomer Kit, Dow Corning). PDMS membranes of 100- $\mu$ m thick were fabricated using a silicon wafer with 100- $\mu$ m diameter posts spaced 400  $\mu$ m apart. The thin PDMS membrane was formed using a spin coater at 3500 rpm for 2 min before scraping over the posts with a glass slide. Partially cured PDMS frames of 0.5 cm (width)  $\times$  0.5 cm (length) (cured for 20 min in an 80 °C oven) were added on top of the fresh PDMS on the mold before curing at 80 °C for 2.5 hr to produce membranes with attached frames.

#### 4.4. Fabrication of Microchannel in Hydrogel

To create microchannel in GelMA/PEG composite hydrogel, molds of 0.25 cm<sup>2</sup> were manufactured from PDMS as described previously<sup>[35]</sup>. Small metal connectors (100- $\mu$ m inner diameter) were punched through the middle of the mold and a sacrificial fiber of 80 $\mu$ m thickness was passed through the connectors. The mold was filled with 80 $\mu$ l of 10% GelMA/2% PEG solution before UV crosslinking for 60 s. These samples were air dried for 12 hr. The PDMS membrane and frame was then plasma bonded on top and PBS was added to allow reswelling of the construct for a number of hours. At this stage the sacrificial fiber was removed to create a microchannel of 80 $\mu$ m diameter through the center of the construct (Fig. 1).

#### 4.5. Fabrication of Hydrogel-coated Thin Microfluidic Device

The device had two parallel and connected channels of 5.5-cm long, 120- $\mu$ m wide, and 150- $\mu$ m high. The devices were fabricated using standard photo- and soft-lithography protocols. Briefly, a master silicon wafer (Silicon Sense, Inc.) was patterned with negative photoresist (SU8-2100, MicroChem Corp.) by spin-coating at 1850 rpm for 40 s, followed by a soft bake (5 min at 65 °C and 22 min at 95 °C) and UV exposure at 260 mJ/cm<sup>2</sup>. These resin-coated wafers were post-exposure baked (5 min at 65 °C and 10 min at 95 °C) and developed using propyleneglycol methyl ether acetate (PGMEA, 484431, Sigma-Aldrich), followed by a 30-min long hardening bake at 180 °C. The microfluidic channels were subsequently generated in 500- $\mu$ m thick PDMS (Sylgard 184, Dow Corning) by spin-coating and further sealed with a porous PDMS membrane described in Section 4.3 using oxygen plasma. To successfully bond the thin microfluidic device, the metal probe was coated by a thin layer of PDMS with 200- $\mu$ m thickness. Thin microfluidic device was then bonded on the PDMS-coated metal probe by oxygen plasma treatment. To connect the microchannel in the device, metal connectors and tygon tubes were used. A 10% GelMA and 2 % PEG solution containing 0.5 w/v% PI in PBS was introduced into the microchannel by a syringe pump at a flow rate 2 mL/hr and was crosslinked under UV light for 3 min at 14.6 mW/cm<sup>2</sup> (Fig. S2). The uncrosslinked GelMA/PEG pre-polymer solution was washed with PBS for 4 min. The entire PDMS structure was sandwiched between two glass plates before exposing to the UV light. The GelMA/PEG-coated devices were stored in PBS for diffusion studies.

Using same method, the thin microfluidic device was coated by 14 % GelMA solution containing 0.8 w/v% PI in PBS.

#### 4.6. Diffusion Studies

For thick microfluidic chip, diffusion was tested optically using FITC-dextran with 20-kDa  $M_W$  as a model for IL-4 ( $M_W$ : 12–20 kDa), 40-kDa  $M_W$  as a model for larger proteins and 389 Da  $M_W$  FITC isomer as a model for DEX ( $M_W$ : 392 Da, Sigma-Aldrich). A solution of 20 mg/mL of FITC-Dextran in PBS was injected into the microchannel until it was full and fluorescent images were taken from above every 5 min at 37 °C. A 100- $\mu$ L reservoir of PBS was added to the top of the PDMS membrane and stored in a humidified chamber in an incubator at 37 °C. Every 24 hr the 100  $\mu$ L was replaced in order to maintain sink conditions and the fluorescence of 2  $\mu$ L of the solution was measured using Nanodrop2000 (Thermo Fisher Scientific). Blank measurements were conducted using PBS and all measurements were completed using triplicates of 2 $\mu$ l samples. FITC-Dextran was measured at 494nm excitation levels and concentrations were calculated using a calibration curve. For the thin microfluidic device on the metal probe, diffusion through the GelMA coating was evaluated using FITC-dextran with a 20-kDa  $M_W$ . A solution of FITC-dextran of 12 mg/mL in PBS was injected inside the microchannel and the images were taken at 0, 30, 60, and 120 s. The fluorescent images were processed using imageJ and the fluorescent intensities across different sections of the channel and different time points were calculated.

#### 4.7. Microscope Imaging

All bright field and fluorescent images were taken on a Zeiss Axio Observer D1 Fluorescence Microscope (Carl Zeiss, Germany) and all scanning electron microscopy images were taken on a Hitachi Model S4700, Japan. Confocal images were taken on Leica SP5X MP, Germany.

#### 4.8. Mechanical properties of Hydrogel

Mechanical properties of the gels were calculated using Instron 5524 mechanical analyzer (Instron, Canton, MA) compressive tests with a 10N load cell. Compressive modulus was calculated between 10 and 20% loading of 600- $\mu$ m thick samples with a 5mm diameter with 6 replicates for each sample.

#### 4.9. Monocyte Culture and Encapsulation

THP-1 monocyte cells (ATCC) were cultured in suspension for at least 7 days before use in Roswell Park Memorial Institute Medium (RPMI) (Life Technologies) supplemented with 10% Fetal Bovine Serum (FBS) (Gibco BRL) and 1% Penicillin-Streptomycin (Gibco BRL) at 0.5–2 million cells/ml media. Cell media was changed every three days, retaining 20% of the old media. Monocytes were encapsulated in 5% GelMA hydrogel with 6 million cells/ml and 50 $\mu$ l of this solution was added on top of the chip and UV crosslinked as before for 20 s.

#### 4.10. Astrocyte Culture and Encapsulation

Primary human astrocytes (ScienceCell) were cultured from in suspension for at least 7 days before use in media (DMEM:F12 with L-glutamine + HEPES, ThermoScientific)

supplemented with 10% FBS (Sigma Aldrich), 10% Astrocyte Growth Supplement (ScienceCell) and 1% Penicillin-Streptomycin (Sigma Aldrich) at 0.5–2 million cells/ml media. Cell media was changed at least every three days, retaining 50% of the old media. Astrocytes were encapsulated in 5% GelMA hydrogel with between 0.1 and 0.5% PI at a density of 1 million cells/ml whereby 50 $\mu$ l of solution was added to the top of the chip and subjected to between 20- and 40-s UV light exposure.

#### 4.11. Chronic Cell Studies

Each sample had an initial infusion of 0.1 mg/mL DEX (Sigma-Aldrich) or 10 ng/mL IL-4 (R&D Systems) through the microchannel, excluding negative controls. Selected samples then had repeated infusions (every 3.5 days) of IL-4 or DEX (Table S1 and S3), with media added every 3.5 days immediately before injections. Immunostaining was carried out at days 7, 14, and 21.

#### 4.12. Live/Dead Assay

Cell viability assays were carried out at days 1 and 7 using Live/Dead kits for mammalian cells (Life Technologies). After washing all samples in warm PBS, a mixed solution of ethidium homodimer-1 and calcein was prepared in a ratio of 4:1 and 300  $\mu$ L of this solution and incubated for 15 min. After this period, samples were washed in PBS five more times, before being left in PBS for microscope imaging.

#### 4.13. Immunostaining

All cell encapsulated hydrogel samples were washed with PBS before fixation in 4% paraformaldehyde (PFA) (Sigma Aldrich) at room temperature for 30 min. Samples were stored overnight at 4°C in PBS at this stage if required. Samples were then incubated in 0.1% Triton x-100 (Sigma Aldrich) at room temperature for 30 min. Blocking was carried out in 1% bovine serum albumin (BSA) (Sigma Aldrich) in PBS at room temperature for 1 hr. For monocyte samples, the primary antibody for CD206 as an M2 macrophage (R&D Systems) was diluted at 1:100 in PBS with 1% BSA and samples were incubated overnight at 4°C in a humidified chamber. The Alexa 488 or Alexa 594 conjugated secondary antibodies (Molecular Probes) were added at a dilution of 1:200 in PBS with 1% BSA and incubated for 1 hr at room temperature in a dark humidified chamber. The primary and secondary antibody addition steps were repeated for 27E10 as an M1 macrophage (R&D Systems) before adding 4, 6-diamidino-2-phenylindole (DAPI, Vector Laboratories Inc.) at 1:1000 dilution for 10 min at room temperature whereby samples were ready for observation under the microscope. Between each stage 3 $\times$ 5min washes in PBS were carried out. For astrocyte samples, DAPI was added at 1:2500 dilution as well as Cellmask 647 membrane stain (Sigma Aldrich) at 1:1000 dilution in a PBS 10% goat serum (Gibco BRL) solution at room temperature for 10 min after which samples were ready for observation under the microscope. Between each stage 3 $\times$ 5min washes in PBS were carried out.

#### 4.14. ELISA Assays

TNF- $\alpha$  and IL-6 sandwich ELISAs (R&D systems) were carried out according to supplier's instructions. Briefly, 50  $\mu$ L of assay diluent and 200  $\mu$ L of sample were added to each well

for 2 hr. Following four washes with the wash buffer, 200  $\mu$ L of either TNF- $\alpha$  or IL-6 conjugate was added and left for a further 2 hr period. After another wash cycle, 200  $\mu$ L of the substrate solution was added and left for 20 min before the addition of a stop solution and the assay was measured at 450 nm and 540 nm using the plate reader.

#### 4.15. Statistical Analysis

All data is expressed as mean  $\pm$  standard deviation. T tests or 2-way ANOVA tests were performed where appropriate with \*  $P < 0.05$  being viewed as significant.

### Supplementary Material

Refer to Web version on PubMed Central for supplementary material.

### Acknowledgments

Laura Frey and Praveen Bandaru contributed equally to this work. This paper was supported by the Institute for Soldier Nanotechnology, National Institutes of Health (HL092836, EB012597, AR057837, HL099073), the National Science Foundation (DMR0847287), ONR PECASE and the Higher Education Authority Ireland. Dr. Su Ryon Shin would like to recognize and thank Brigham and Women's Hospital President Betsy Nabel, MD, and the Reny family, for the Stepping Strong Innovator Award through their generous funding. Many thanks to Fulbright Ireland Association for further funding and facilitating this collaboration between Trinity and Harvard-MIT Health Sciences.

### 5. References

- [1]. a)Massia SP, Holecko MM, Ehteshami GR, J Biomed Mater Res A 2004, 68, 177; [PubMed: 14661263] b)Polikov VS, Tresco PA, Reichert WM, J Neurosci Methods 2005, 148, 1; [PubMed: 16198003] c)Udupa K, Chen R, Prog Neurobiol 2015, 133, 27. [PubMed: 26296674]
- [2]. a)R. V. B, SB P, P. R, MRS Bull 2012, 37(06), 557;b)W H, GC M, TM S, RV B, Adv Mater. 2007, 19(21), 3529.
- [3]. a)Y L, D W, T. L et al., Biomaterials 2009, 30(25), 4143; [PubMed: 19467702] b)Yue Z, Moulton SE, Cook M, O'Leary S, Wallace GG, Adv Drug Deliv Rev 2013, 65, 559; [PubMed: 22705546] c)Rao L, Zhou H, Li T, Li C, Duan YY, Acta Biomater 2012, 8, 2233. [PubMed: 22406507]
- [4]. a)Pieperhoff S, Front Physiol 2012, 3, 1; [PubMed: 22275902] b)He W, Bellamkonda RV, Biomaterials 2005, 26, 2983; [PubMed: 15603793] c)Bergey GK, Exp Neurol 2013, 244, 87. [PubMed: 23583414]
- [5]. LR H, D B, e. a. Jarosiewicz B, Nature 2012, 485(7398), 372. [PubMed: 22596161]
- [6]. a)Green RA, Lovell NH, Wallace GG, Poole-Warren LA, Biomaterials 2008, 29, 3393;b)Jiang LL, Liu JL, Fu XL, Xian WB, Gu J, Liu YM, Ye J, Chen J, Qian H, Xu SH, Pei Z, Chen L, Chin Med J (Engl) 2015, 128, 2433. [PubMed: 26365958]
- [7]. Bjornsson CS, Oh SJ, Al-Kofahi YA, Lim YJ, Smith KL, Turner JN, De S, Roysam B, Shain W, Kim SJ, J Neural Eng 2006, 3, 196. [PubMed: 16921203]
- [8]. a)Szarowski DH, Andersen MD, Retterer S, Spence AJ, Isaacson M, Craighead HG, Turner JN, Shain W, Brain Res 2003, 983, 23; [PubMed: 12914963] b)R B, DC M, PA T, J Biomed Mater Res A 2007, 169.
- [9]. a)A. W. McCreery DB, Yuen TG, Bullara L., IEEE Trans Biomed Eng 1990, 37(10), 996; [PubMed: 2249872] b)Liu H, Zhu L, Sheng S, Sun L, Zhou H, Tang H, Qiu T, J Neural Eng 2013, 10, 036024. [PubMed: 23676976]
- [10]. Potter KA, Jorfi M, Householder KT, Foster EJ, Weder C, Capadona JR, Acta Biomater 2014, 10, 2209. [PubMed: 24468582]
- [11]. a)Szarowski DH, Andersen MD, Retterer S, Spence AJ, Isaacson M, Craighead HG, Turner JN, Shain W, Brain Res 2003, 983, 23; [PubMed: 12914963] b)Potter KA, Jorfi M, Householder KT, Foster EJ, Weder C, Capadona JR, Acta Biomater 2014, 10, 2209. [PubMed: 24468582]

- [12]. Turner JN, Shain W, Szarowski DH, Andersen M, Martins S, Isaacson M, Craighead H, Experimental Neurology 1999, 156, 33. [PubMed: 10192775]
- [13]. a)Liu W, Tang Y, Feng J, Life sciences 2011, 89, 141; [PubMed: 21684291] b)Yamasaki R, Lu H, Butovsky O, Ohno N, Rietsch AM, Cialic R, Wu PM, Doykan CE, Lin J, Cotleur AC, Kidd G, Zorlu MM, Sun N, Hu W, Liu L, Lee JC, Taylor SE, Uehlein L, Dixon D, Gu J, Floruta CM, Zhu M, Charo IF, Weiner HL, Ransohoff RM, J Exp Med 2014, 211, 1533. [PubMed: 25002752]
- [14]. a)Ravikumar M, Sunil S, Black J, Barkauskas DS, Haung AY, Miller RH, Selkirk SM, Capadona JR, Biomaterials 2014, 35, 8049; [PubMed: 24973296] b)Cherry JD, Olschowka JA, O'Banion MK, J Neuroinflammation 2014, 11, 98; [PubMed: 24889886] c)Franco R, Fernandez-Suarez D, Prog Neurobiol 2015, 131, 65. [PubMed: 26067058]
- [15]. Zhong Y, Bellamkonda RV, Brain Res 2007, 1148, 15. [PubMed: 17376408]
- [16]. Nichol JW, Koshy ST, Bae H, Hwang CM, Yamanlar S, Khademhosseini A, Biomaterials 2010, 31, 5536. [PubMed: 20417964]
- [17]. a)Yue K, Trujillo-de Santiago G, Alvarez MM, Tamayol A, Annabi N, Khademhosseini A, Biomaterials 2015, 73, 254; [PubMed: 26414409] b)Coimbra P, Gil MH, Figueiredo M, Int J Biol Macromol 2014, 70, 10. [PubMed: 24971558]
- [18]. a)Simmons A, Padsalgikar AD, Ferris LM, Poole-Warren LA, Biomaterials 2008, 29, 2987; [PubMed: 18436300] b)Agarwal A, Goss JA, Cho A, McCain ML, Parker KK, Lab Chip 2013, 13, 3599. [PubMed: 23807141]
- [19]. Hutson CB, Nichol JW, Aubin H, Bae H, Yamanlar S, Al-Haque S, Koshy ST, Khademhosseini A, Tissue engineering. Part A 2011, 17, 1713. [PubMed: 21306293]
- [20]. Budday S, Nay R, de Rooij R, Steinmann P, Wyrobek T, Ovaert TC, Kuhl E, J Mech Behav Biomed Mater 2015, 46, 318. [PubMed: 25819199]
- [21]. Huang S-H, Lin S-P, Chen J-J, Sensors and Actuators A: Physical 2014, 216, 257.
- [22]. Joint C, Nandi D, Parkin S, Gregory R, Aziz T, Mov Disord 2002, 17 Suppl 3, S175. [PubMed: 11948774]
- [23]. a)Kim D-H, Martin DC, Biomaterials 2006, 27, 3031; [PubMed: 16443270] b)Spataro L, Dilgen J, Retterer S, Spence AJ, Isaacson M, Turner JN, Shain W, Experimental Neurology 2005, 194, 289. [PubMed: 16022859]
- [24]. a)Michelucci A, Heurtaux T, Grandbarbe L, Morga E, Heuschling P, Journal of neuroimmunology 2009, 210, 3; [PubMed: 19269040] b)McWhorter FY, Wang T, Nguyen P, Chung T, Liu WF, Proc Natl Acad Sci U S A 2013, 110, 17253. [PubMed: 24101477]
- [25]. Losciuto S, Dorban G, Gabel S, Gustin A, Hoenen C, Grandbarbe L, Heuschling P, Heurtaux T, J Neurosci Methods 2012, 207, 59. [PubMed: 22483759]
- [26]. a)Wilcock DM, Int J Alzheimers Dis 2012, 2012, 495243; [PubMed: 22844636] b)Polazzi E, Monti B, Prog Neurobiol 2010, 92, 293; [PubMed: 20609379] c)Sawyer AJ, Tian W, Saucier-Sawyer JK, Rizk PJ, Saltzman WM, Bellamkonda RV, Kyriakides TR, Biomaterials 2014, 35, 6698. [PubMed: 24881026]
- [27]. Ito C, Evans WE, McNinch L, Coustan-Smith E, Mahmoud H, Pui CH, Campana D, J Clin Oncol 1996, 14, 2370. [PubMed: 8708730]
- [28]. Tedesco S, Bolego C, Toniolo A, Nassi A, Fadini GP, Locati M, Cignarella A, Immunobiology 2015, 220, 545. [PubMed: 25582402]
- [29]. Knopf-Marques H, Singh S, Htwe SS, Wolfova L, Buffa R, Bacharouche J, Francius G, Voegel JC, Schaaf P, Ghaemmaghami AM, Vrana NE, Lavalley P, Biomacromolecules 2016, 17, 2189. [PubMed: 27183396]
- [30]. Placone AL, McGuiggan PM, Bergles DE, Guerrero-Cazares H, Quinones-Hinojosa A, Searson PC, Biomaterials 2015, 42, 134. [PubMed: 25542801]
- [31]. Frankola KA, Greig NH, Luo W, Tweedie D, CNS Neurol Disord Drug Targets 2011, 10, 391. [PubMed: 21288189]
- [32]. Karumbaiah L, Saxena T, Carlson D, Patil K, Patkar R, Gaupp EA, Betancur M, Stanley GB, Carin L, Bellamkonda RV, Biomaterials 2013, 34, 8061. [PubMed: 23891081]
- [33]. Annabi N, Selimovic S, Acevedo Cox JP, Ribas J, Afshar Bakooshli M, Heintze D, Weiss AS, Cropek D, Khademhosseini A, Lab Chip 2013, 13, 3569. [PubMed: 23728018]

- [34]. Van Den Bulcke AI, Bogdanov B, De Rooze N, Schacht EH, Cornelissen M, Berghmans H, Biomacromolecules 2000, 1, 31. [PubMed: 11709840]
- [35]. Annabi N, Shin SR, Tamayol A, Miscuglio M, Bakooshli MA, Assmann A, Mostafalu P, Sun JY, Mithieux S, Cheung L, Tang XS, Weiss AS, Khademhosseini A, Adv Mater 2016, 28, 40. [PubMed: 26551969]

Author Manuscript

Author Manuscript

Author Manuscript

Author Manuscript



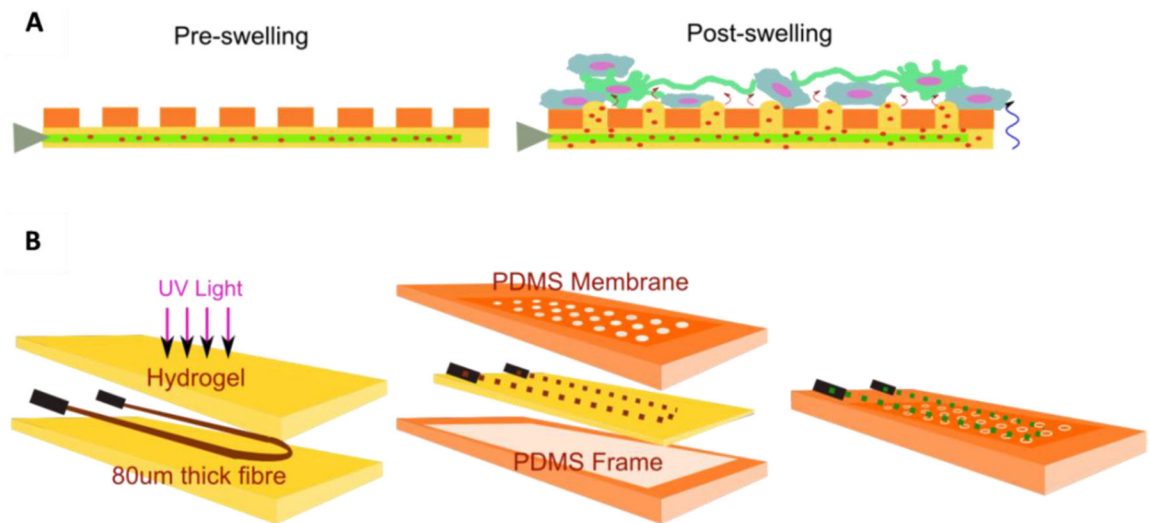


**Figure 1.** Construction of dual-layered microfluidic system and its concept. A) Schematic diagram illustrating the concept of the transformation from dry insertion state to drug delivering implantation state. B) Preparation procedure of microchannel in GeIMA/PEG hydrogel construct surrounded by a microporous PDMS membrane.

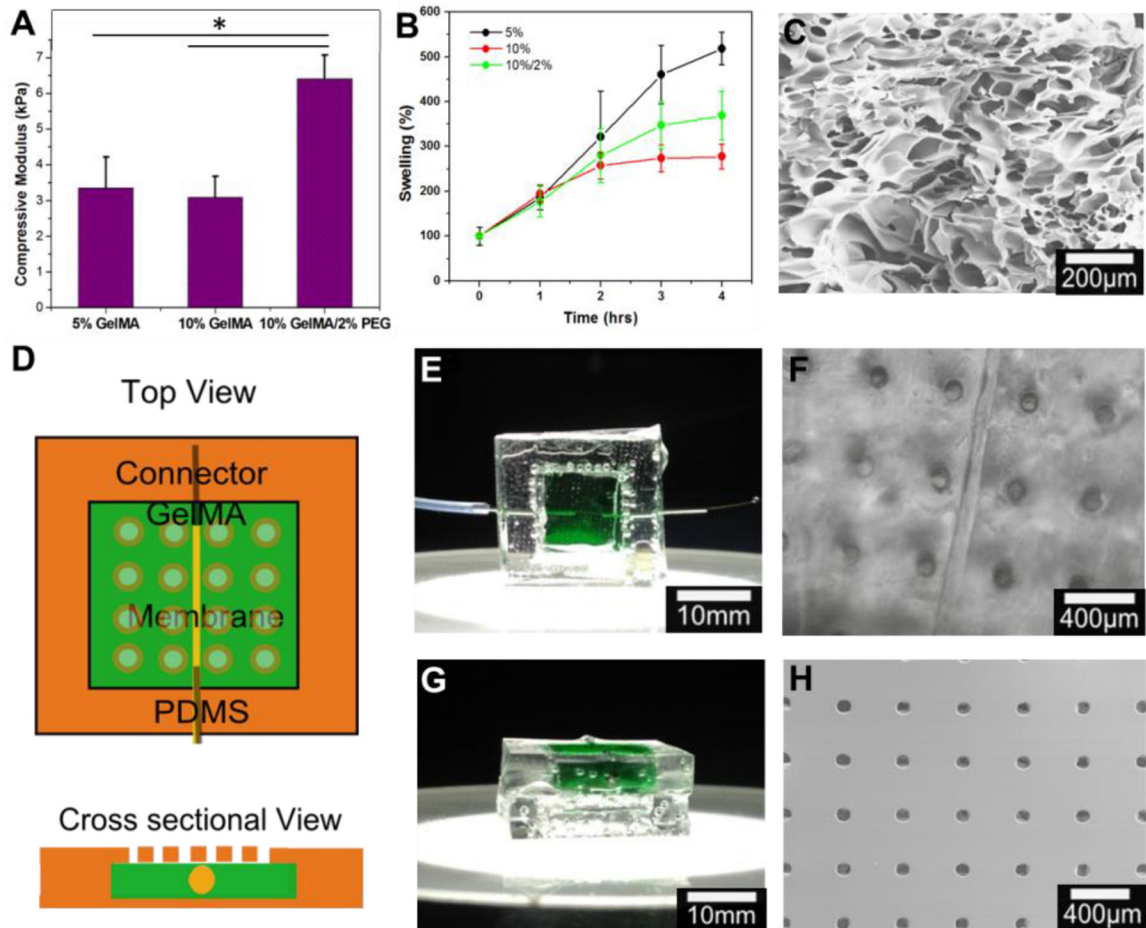


**Figure 2.** Chip design optimization. A) Compressive modulus of three different concentrations of GelMA/PEG hydrogel composites (\*  $P < 0.05$ ). B) Reswelling profiles of three different concentrations of GelMA/PEG hydrogel composites (\*  $P < 0.05$ ). C) Microstructure of GelMA/PEG composite hydrogel captured using scanning electron microscopy. D) Schematic of chip design E) Top view of sample chip with GelMA/PEG composite hydrogel section stained green. F) Optical image of top view of chip showing 100  $\mu\text{m}$  channel and 100  $\mu\text{m}$  pores. G) Cross-sectional view of sample chip with GelMA/PEG section stained green. H) Scanning electron microscope image of PDMS membrane with 100  $\mu\text{m}$  pores with 400  $\mu\text{m}$  spacing.

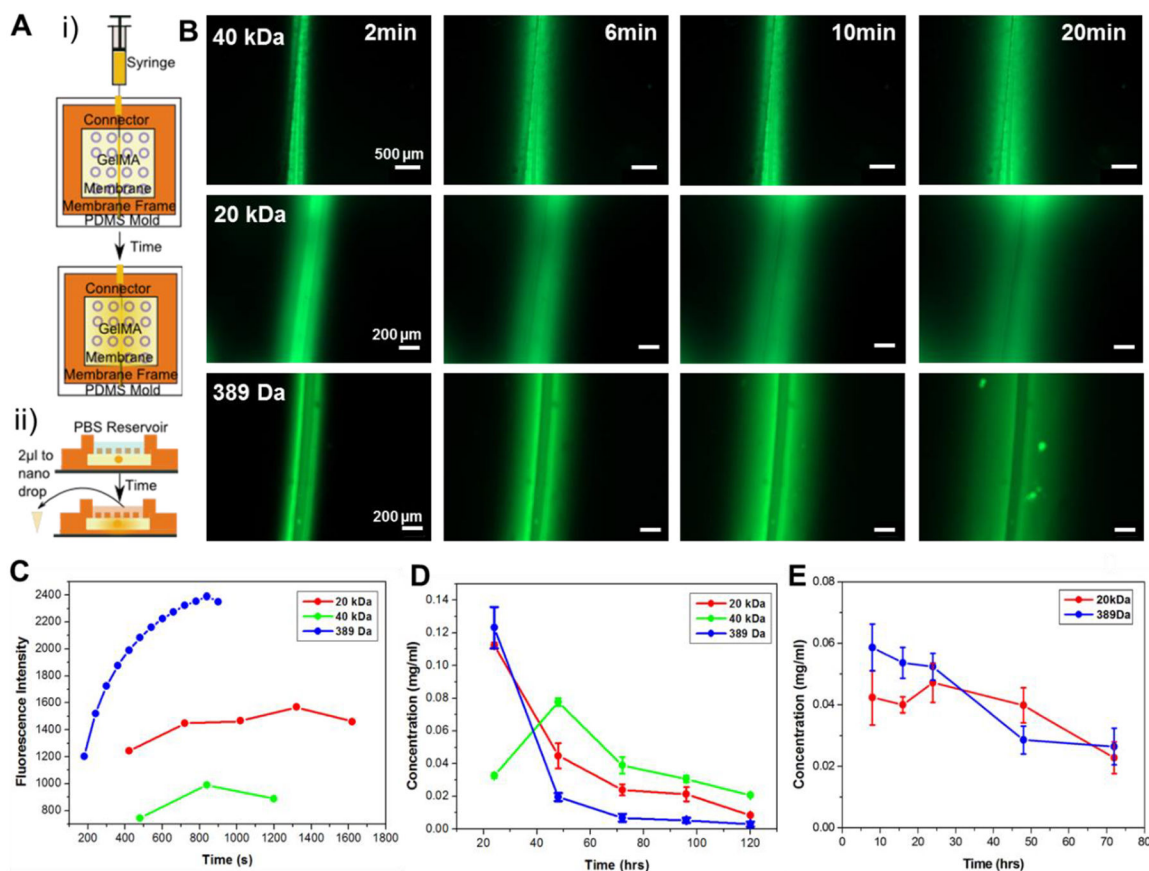


**Figure 3.** Diffusion profiles of FITC variants with different molecular weights through chip system. A) Schematic of tests to show diffusion: i) optical set-up using microscope images and ii) quantification using nanodrop to measure diffusion into a PBS reservoir. B) Fluorescence images over time of FITC-Dextran (40-kDa  $M_w$  and 20-kDa  $M_w$  respectively) and FITC isomer (389-Da  $M_w$ ) showing effect of molecular weight on diffusion time. C) Progression of fluorescent signal at a point 100 $\mu$ m away from microchannel as FITC diffuses through hydrogel system. D) Concentration of FITC isomer and -dextran with different molecular weights diffused through the porous PDMS membrane into PBS reservoir at 24 hr time points. E) Concentration of FITC isomer and -dextran with different molecular weights diffused through the porous PDMS membrane into PBS reservoir at 8 hr time points.

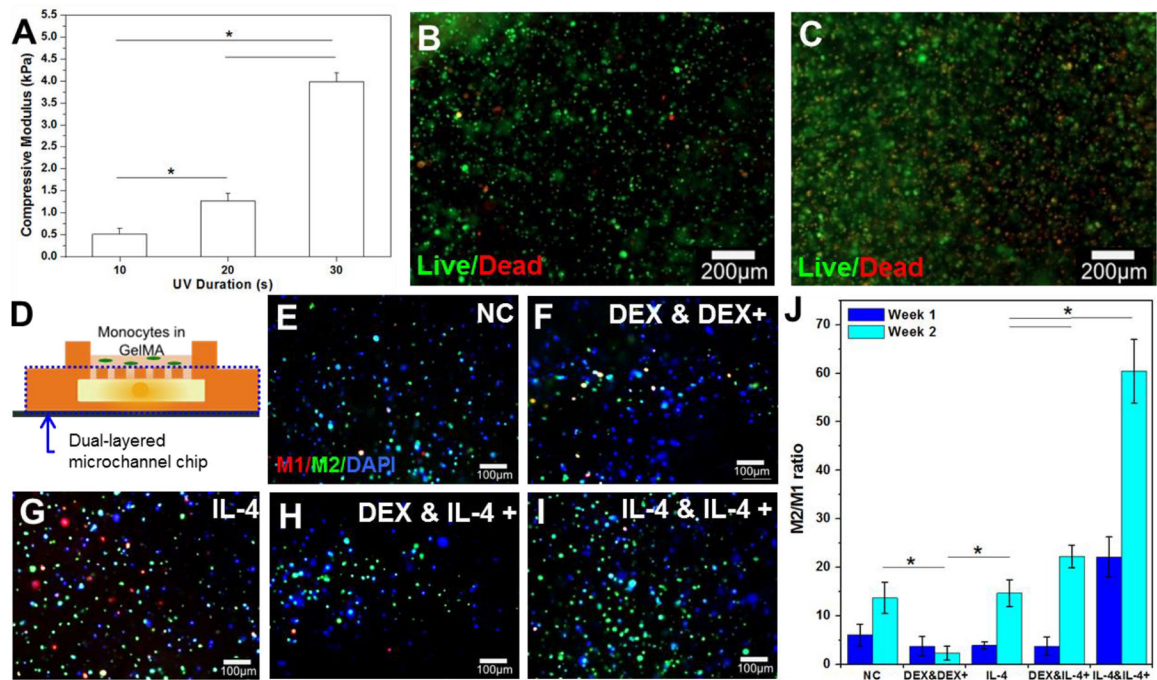


**Figure 4.**

Phenotype of monocyte cells encapsulated in the 5% GelMA system as an *in vitro* model for brain immune response after different drug delivery profiles were delivered through the dual-layered microchannel chip system. A) Compressive modulus of monocytes encapsulated in 5% GelMA hydrogel with various UV time (\*  $P < 0.05$ ). B) and C) Fluorescent images of monocytes stained using calcein (green) for live cells and ethidium homodimer-1 (red) for dead cells at day 0 (B) and day 7 (C). D) Schematic of experimental set-up showing monocytes encapsulated in GelMA hydrogel on top of the dual-layered microchannel chip. E) – I) Immunostaining of CD206 (green) as an M2 macrophage, nuclei (blue), and 27E10 (red) as an M1 macrophage for samples with: E) no infusions (negative control); F) an initial DEX infusion and repeated DEX infusions; G) an initial IL-4 infusion only; H) an initial DEX infusion and repeated IL-4 infusions; I) an initial IL-4 infusion and repeated IL-4 infusions at week 1. J) Ratio of M2:M1 differentiated macrophages for all delivery profiles at 1 and 2 weeks indicating that repeated infusion of IL-4 significantly increases the presence of anti-inflammatory M2 macrophages (\*  $P < 0.05$ ).

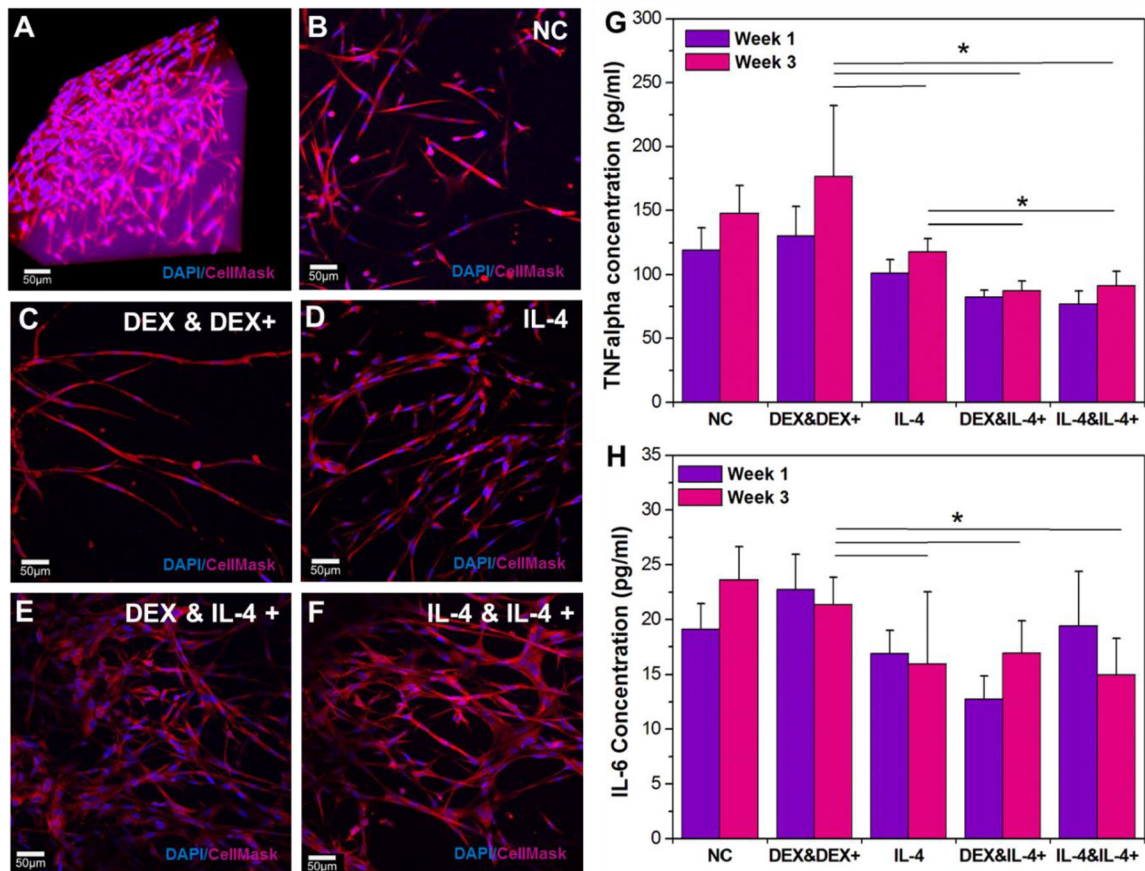


**Figure 5.**

Confocal stacks images of hydrogel-encapsulated astrocytes after 3 weeks of different drug delivery profiles from the dual-layered microfluidic chip system. A) A 3D reconstruction image of optimized 3D astrocyte models with DAPI staining (blue) for nuclei and Cell Mask 649 (red) for cell structure at week 1. Chronic study samples with: B) no infusions (negative control); C) an initial DEX infusion and repeated DEX infusions; D) an initial IL-4 infusion only; E) an initial DEX infusion and repeated IL-4 infusions; F) an initial IL-4 infusion and repeated IL-4 infusions; G) Pro-inflammatory marker TNF- $\alpha$  release for each profile at week 1 and 3 (\*  $P < 0.05$ ). H) Pro-inflammatory marker IL-6 release for each profile at week 1 and 3 (\*  $P < 0.05$ ).

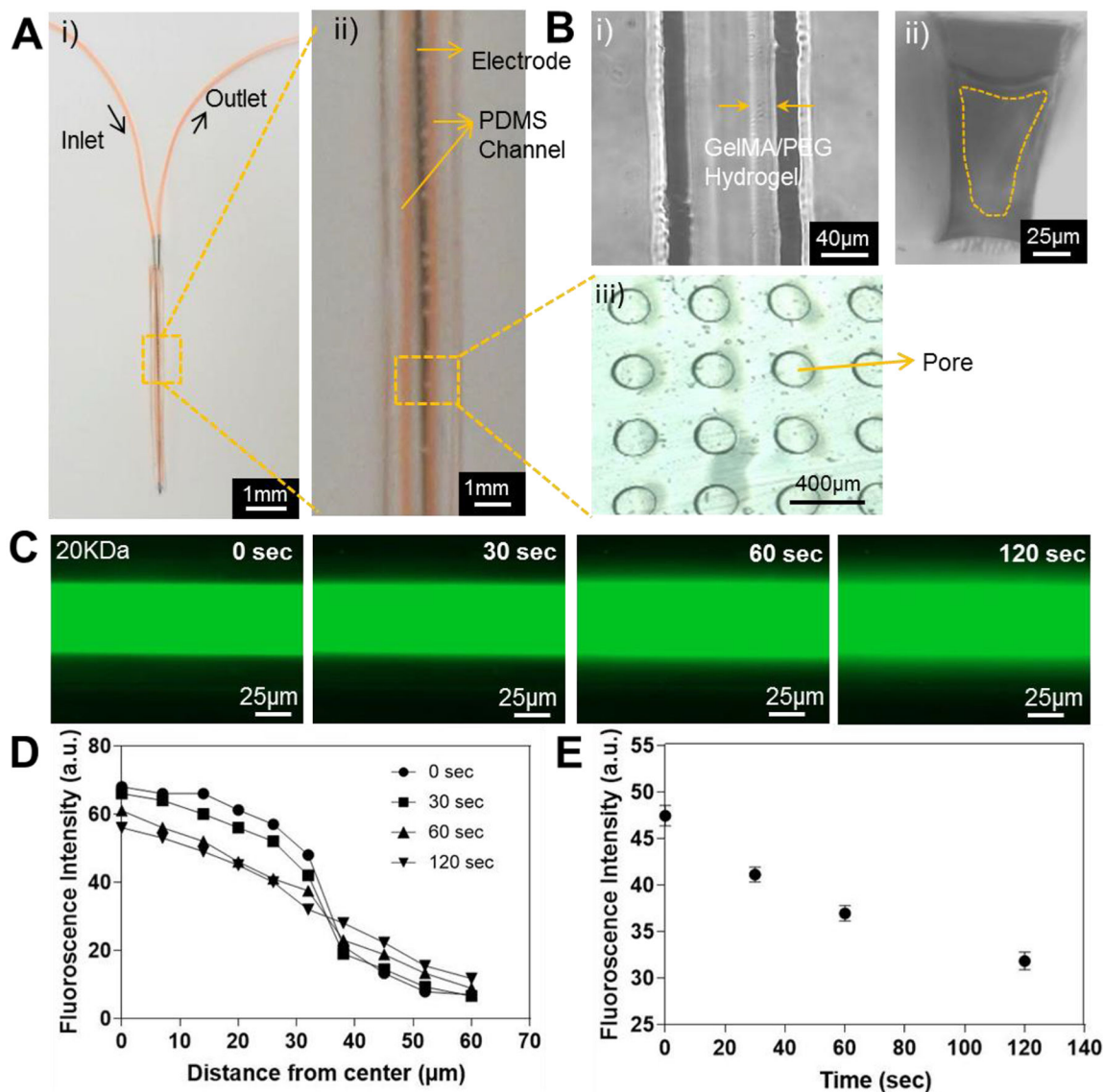


**Figure 6.**

A) The thin dual-layered microfluidic device integrated on a metal probe. i) Top view and ii) magnified top view with microchannel in orange color. B) Brightfield image of the GelMA/PEG hydrogel coating inside the microchannel. i) Top view; ii) cross-sectional view; and iii) porous PDMS membrane. C) Fluorescence images showing the diffusion of FITC-dextran (20-kDa  $M_w$ ) at different time points. D) Quantification of fluorescence intensities measured from the middle to the side along its radius of the microchannel at different time points. E) Time-lapse fluorescent signal change at a point 30 µm from the middle of the microchannel.